4.9 GLOBAL MEASUREMENTS OF WIND USING COMPLEX SYNTHETIC APERTURE RADAR IMAGES

S. Lehner[1], J. Horstmann[2], J. Schulz-Stellenfleth[1], M. Bao[1], and W. Koch[2]

[1]German Aerospace Center, Oberpfaffenhoven, Germany
[2]GKSS Research Center, Geesthacht, Germany

ABSTRACT: A global set of single look complex (SLC) synthetic aperture radar (SAR) images is processed, using the B-SAR processor developed at the German Aerospace Center (DLR). The imgages were focused from wave mode raw data, which where acquired by the European remote sensing satellite ERS-2. Every day about 1000 SAR images of 5 km × 10 km size every 200 km along the satellite track are available thus yielding global and continuous coverage of the oceans. This dataset is used to derive wind speed and direction. The wind speed is derived from the empirical C-band model CMOD4 using the mean normalized radar cross section of the image together with additional information on wind direction. Wind directions are derived from wind streaks visible on images or respective ERS-2 SCAT measurements. Global comparison to model results of the European Center for Medium Range Weather Forecast (ECMWF) and ERS-2 SCAT measurements is performed.

1. INTRODUCTION

Due to their all weather capability and high resolution, synthetic aperture radar (SAR) systems have become a valuable measurement tool for marine parameters like wind speed [1], [2], and [3] and [4] (this issue), ocean wave spectra [5], and sea ice parameters [6].

Since the launch of the ERS-1 and ERS-2 satellites of the European Space Agency (ESA) in 1991 and 1995, synthetic aperture radar (SAR) images have been acquired over the oceans on a continuous basis. Full swath scenes of 100 km × 100 km size are taken where receiving stations are in line of sight, whereas 5 km × 10 km images are acquired every 200 km along the orbit and therefore yield global and continuous observations.

To take advantage of the full high resolution image information ERS-2 wave mode raw data were processed to single look complex SAR imagettes, that are not available as a standard ESA product, using the BSAR processor, developed at the German Space Agency. In total $34\,310$ SAR imagettes were processed representing 27 days of data between August 21, 1996 and June 2, 1997. Studies on the use of ERS wave mode data for wind measurements were already published by [7] and [8]. However, a rigorous calibration and subsequent determination of wind speeds has not been undertaken until now. This paper aims at developing a SAR wind retrieval algorithm for the global ERS-2 SAR wave mode data set. Wind direction is retrieved from wind induced streaks and wind speed from the mean normalized radar cross section of the SAR imagette using the C-band model CMOD4, which was originally developed for the ERS scatterometer (SCAT) [9].

In general this study is a preparation for the new data products available from the advanced SAR (ASAR) of the European Environmental satellite (ENVISAT) to be launched in 2001. As ENVISAT will not carry a scatterometer, the development of ASAR wind measurement techniques is of special interest.

2. DATA

In SAR wave mode the ERS satellite acquires images every 200 km along the orbit at a nominal incidence angle of $23°$. SAR wave mode data cover a region of 10 km in range and 5 km in azimuth with a spatial resolution of ~ 30 m. In contrast to the SAR image mode, SAR wave mode data rates allow continuous and global operation with simultaneous acquisition of SCAT data. Unfortunately, ESA does not offer these data as single look complex SAR data so that a data set consisting of $34\,310$ representing 27 days of data between August 21, 1996 and June 2, 1997 were processed at the German Aerospace Center (DLR) to so called SAR imagettes [8] using their processor BSAR. Fig. 1 shows examples of different imagettes with ocean wave (d) and others with that show features caused by atmospheric effects (e,f) or sea ice (a, b, c).

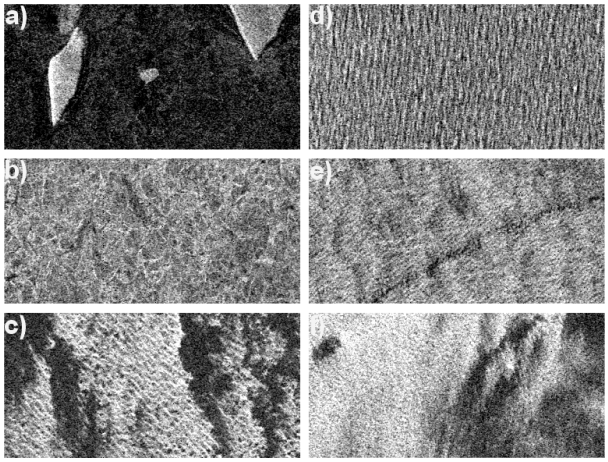

Fig. 1: Examples of ERS-2 SAR imagettes showing different features such as different types of ice (a, b and c) ocean waves (c and d) and atmospheric features (d, e and f).

In addition to the SAR imagettes collocated ERS-2 SCAT wind measurements were available which were processed at the French ERS processing and archiving facility in Brest Centre ERS d'archivage et de traitement (CERSAT) using the C-band model CMOD_IFR2. These data have an accuracy of 15° in wind direction and 1.2 ms^{-1} in wind speed [10]. Furthermore, collocated wind information is available from the numerical atmospheric model T213L31 of the European center for medium range weather forecast (ECMWF). The ECMWF model winds are available every 6

h at a spatial resolution of 1°. Both 6 h forecast and analysis data are used for comparison to satellite measurements. Details on the assimilation procedure and input data used for the analysis are provided in [11].

3. SAR RETRIEVED WIND DIRECTIONS

Wind directions can be retrieved from the direction of wind induced streaks visible in most SAR images e.g. from boundary layer rolls, Langmuir cells, or wind shadowing, which are approximately in line with the mean wind direction [12].

Fig. 2 shows the mean variance spectrum (solid line) of ERS wave mode data calculated by averaging over a global data set of 3000 imagettes. The dashed lines indicate the $\pm 0.25\sigma$ interval. It can be seen that the image variance is dominated by shorter waves below wavelength of about 600 m. On average waves longer than 600 m contribute about 5% to the total variance. Wind streaks are found on the longer spatial scale and are thus a relatively weak pattern compared to the short scale image modulation, which is mainly due to ocean surface waves. For this reason the first step in wind streak detection is to filter short waves. In this study a separation wave length of 900 m was chosen as in this wave length regime a weak local minimum can be found in the average variance spectrum. This finding is also consistent with the observation that ocean waves of such length are very rarely seen, so that they are often neglected in ocean wave models. The dashed dotted line in Fig. 2 indicates the speckle noise contribution to the SAR image variance if a single look imagette is used. As speckle is white noise it adds variance to all wavenumbers including the wind streak scale. To remove the speckle contribution the so called multi look technique is used, where two looks with uncorrelated speckle are processed from complex SAR data. It can be shown that the cross spectrum of the two looks is not biased by speckle in contrast to the conventional SAR image power spectrum. For this reason the SAR cross

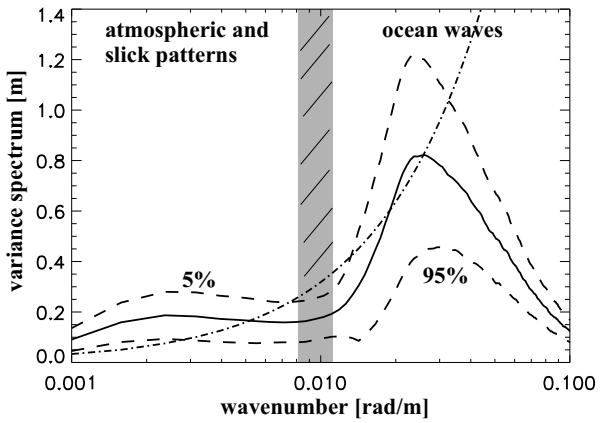

Fig. 2: Mean variance spectrum computed from a global dataset of 3000 ERS wave mode imagettes (solid line). The speckle contribution was removed by multi look techniques. Dashed lines indicate $\pm 0.25\sigma$ interval. The dashed dotted line gives the speckle contribution resulting for a single look SAR image.

spectrum is used as basis for wind streak estimation.

By inspection it was found that in many cases wind streaks show a periodic behaviour so that they can to first order be modeled by plain harmonic waves. Wind streak detection then becomes a simple spectral estimation problem. To remove the short waves a low pass filter is applied to the cross spectrum. Subsequently the maximum of the cross spectrum modulus is searched for. The direction of the maximum indicates the direction of the dominant harmonic wave on the long spatial scale. Wind direction is assumed to be perpendicular to the spectral peak direction. Due to the symmetry of the spectrum, the wind direction can only be estimated with a 180° ambiguity.

The algorithm for wind direction retrieval was applied to 10147 SAR imagettes acquired between 60°N and 60°S. The threshold was selected to exclude SAR imagettes containing sea ice. In 5064 of the 10147 SAR imagettes considered wind streaks were detected by the algorithm and in 3268 of these the wind direction agreed better than 30° to the ERS-2 SCAT measurements. In Fig. 3. the wind

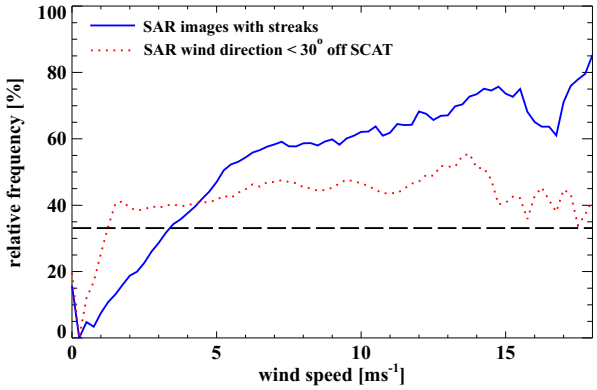

Fig. 3: Wind speed from ERS-2 SCAT versus relative frequency of wind streaks (solid line) and wind directions from SAR imagettes that agree better than 30° to ERS-2 SCAT wind directions (dotted line).

speeds measured by ERS-2 SCAT are plotted versus relative frequency of wind streaks (solid line) and SAR retrieved wind directions that agree better than 30° when compared to ERS-2 SCAT wind directions (dotted line). The dashed line in Fig. 3 results if SCAT wind directions and streak orientations are assumed to be uncorrelated and uniformly distributed. It can be seen that for wind speeds higher than 5 ms^{-1} wind streaks can be detected on more than 50% of all images.

4. SAR RETRIEVED WIND SPEEDS

The method for wind speed retrieval is based on an empirical model relating the wind vector to the normalized radar cross section (NRCS). The most popular model is the CMOD4 model [13] that relates the NRCS of the ocean surface to the near surface wind and incidence angle. It has been shown in previous studies that CMOD4 can be applied to well calibrated SAR images e.g. [1], [2], [14] and [4] (this issue).

So far SAR wave mode imagettes are not calibrated for NRCS and there are no calibration information available, such as a calibration constant, power loss look up table, or antenna pattern. However, to apply CMOD4 to SAR imagettes their amplitudes have to be accurately calibrated and transformed to NRCS. Most of the SAR calibration parameters are incidence angle dependent. However, due to the small range of incidence angles in SAR wave mode imagettes ($\sim 0.7°$) this dependency can be neglected and the NRCS can be approximated by

$$\text{NRCS} = A^2 \cdot k_{im} \text{ power loss}_{im}, \qquad (1)$$

where A is the amplitude, k_{im} the calibration constant including a constant for the range spreading loss and power loss$_{im}$ is the power loss for SAR images caused by analogue to digital (AD) converter saturation. Normally the calibration constant is estimated from corner reflector measurements, which are not available for the collected SAR imagettes. Hereafter, the CMOD4 which describes the dependency of NRCS on the wind vector and incidence angle is used for calibration of NRCS. Therefore, the calibration constant is estimated from the difference of mean SAR image intensity to CMOD4 retrieved NRCS. As input to the CMOD4 wind direction from the ERS-2 SCAT measurements is used together with an incidence angle of 23°. To exclude SAR images affected by sea surface manifestations not caused by the wind, e.g., sea surface slicks, and imagettes that are affected by power loss, only SAR imagettes in the range of 5 to 8 ms^{-1} were considered. The resulting calibration constants is -45.0334 dB.

The power loss correction, which is dependent on the mean SAR amplitude, can be estimated in a similar manner as the calibration constant. Therefore, power loss affected NRCS of all SAR imagettes are derived considering only the amplitude and calibration constant. Again the expected NRCS of each SAR imagette is retrieved by using the CMOD4 considering imagettes with wind speeds above 5 ms^{-1}. The differences between the expected and power loss affected NRCS give an estimate of power loss for each SAR imagette. To get a function of the power loss a polynomial was fitted to the differences between the expected and power loss affected NRCS. However, due to the small number of imagettes acquired at wind speeds higher than 15 ms^{-1} the estimated power loss correction at high NRCS's is uncertain.

To retrieve wind speed from SAR images the mean NRCS was derived according to eq. (1). Wind speed was derived by CMOD4 using as input the NRCS, a fixed incidence angle of 23° and wind directions either from the collocated ECMWF model or ERS-2 SCAT measurements. In Fig. 4 the results of the comparison of wind speed from ERS-2 SCAT versus SAR-retrieved wind speed are plotted considering all collocations between $60°$N and $60°$S and the wind directions from ERS-2 SCAT. The corresponding main statistical parameters are plotted in the upper left of the plot. The correlation is 0.94.

Comparison of SAR derived wind speed to ECMWF forecast and to ECMWF analysis shows a slightly lower correlation of

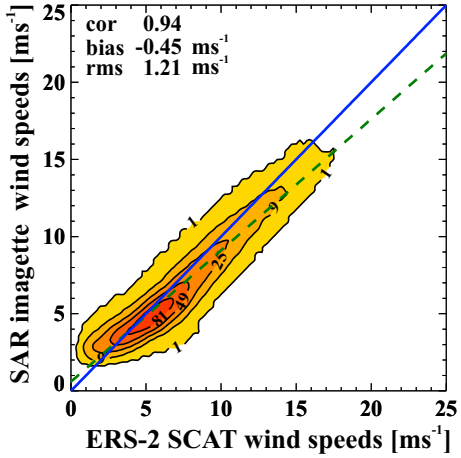

Fig. 4: Wind speeds from ERS-2 SCAT versus wind speeds retrieved from SAR imagettes using CMOD4 considering ERS-2 SCAT wind directions.

0.87 and 0.85 respectively, with a bias of 0.32 ms^{-1} and 0.6 ms^{-1} and a root mean square error of 1.69 ms^{-1} and 1.81 ms^{-1}. It is interesting to note that although the ECMWF analysis data contain ERS SCAT winds correlation does not improve. Comparison to ERS-2 SCAT wind speeds show a significant better agreement, which is due to the similarity of both instruments and the exact collocation in time.

However, comparison to ERS-2 SCAT retrieved wind speeds shows an overestimation for wind speeds below 5 ms^{-1}. This is due to a further AD-conversion problem caused by a too low input signal to the AD-converter causing bit redundancy which in turn leads to a power gain and therefore to an overestimation of wind speed. To get a more accurate correction of the AD-converter errors (power loss and power gain) SAR imagette RAW data have to be analyzed according to the method described by Meadows et al. [15].

Fig. 5 shows a world map of wind vectors from Sep 5, 1996. The wind speed was derived from SAR imagettes using the wind direction from ECMWF model data.

5. CONCLUSIONS

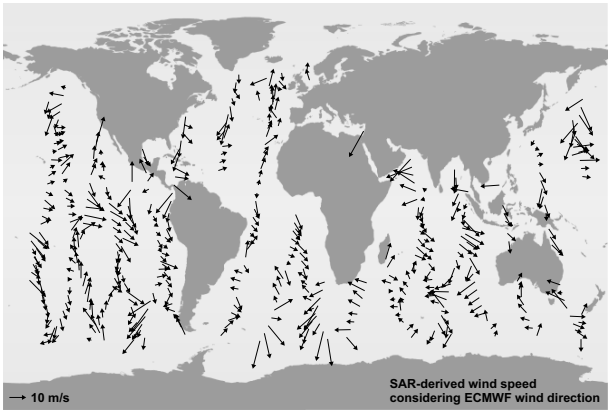

Fig. 5: World map showing wind vectors from September 5, 1996. The wind speeds were derived from SAR imagettes using the wind direction from ECMWF model data.

A new data set, complex ERS-2 SAR wave mode data, was used to derive wind speed and direction on a global scale. Results were compared to collocated ERS-2 SCAT wind speed measurements and ECMWF atmospheric model data.

A method based on complex SAR data is presented to derive wind direction from wind streaks found on imagettes. It was shown that the agreement of SAR derived wind direction to SCAT measurements increases with increasing wind speed.

A calibration procedure was derived based on a linear regression between mean image intensity and collocated SCAT wind speed. In addition, a power loss correction was estimated.

Wind speed was derived from the calibrated SAR imagettes using the CMOD4 method with ECMWF wind directions used as additional input.

ACKNOWLEDGMENTS

The authors were supported by the German Bundesministerium für Bildung und Forschung (BMBF) in the framework of the project ENVOC. The ERS-2 SAR wave mode raw data were kindly provided by the European Space Agency (ESA) as part of AO3 COMPLEX 714.

References

[1] P. W. Vachon and F.W. Dobson, "Validation of wind vector retrieval from ERS-1 SAR images over the ocean," *The Global Atm. and Ocean Syst.*, vol. 5, pp. 177–187, 1996.

[2] S. Lehner, J. Horstmann, W. Koch, and W. Rosenthal, "Mesoscale wind measurements using recalibrated ERS SAR images," *J. Geophys. Res.*, vol. 103, pp. 7847–7856, 1998.

[3] J. Horstmann, W. Koch, S. Lehner, and R. Tonboe, "Mesoscale wind fields retrieved from RADARSAT-1 ScanSAR in view of ENVISAT ASAR," in *in Proceedings of ERS ENVISAT SYMPOSIUM (this issue)*, Gothenburg, Sweden, 2000.

[4] J. Horstmann, W. Koch, S. Lehner, and R. Toboe, "An algorithm for operational wind field retrieval using RADARSAT-1 ScanSAR images," in *in Proceedings of AMS (this issue)*, San Diego, USA, 2001.

[5] P. Heimbach, S. Hasselmann, and K. Hasselmann, "Statistical analysis and intercomparison with WAM model data of three years of global ERS-1 SAR wave Mode Spectral retrievals," *J. Geophys. Res.*, vol. 103, pp. 7931–7977, 1998.

[6] J. Schulz-Stellenfleth and S. Lehner, "Sea surface imaging with an across track interferometric synthetic aperture radar — the sinewave experiment," *J. Geophys. Res.*, submitted 2001.

[7] V. Kerbaol, B. Chapron, and P. W. Vachon, "Analysis of ERS-1/2 synthetic aperture radar wave mode imagettes," *J. Geophys. Res.*, vol. 103, pp. 7833–7846, 1998.

[8] S. Lehner, J. Schulz-Stellenfleth, B. Schättler, H. Breit, and J. Horstmann, "Wind and wave measurements using complex ERS-2 SAR wave mode data," *IEEE Trans. Geosci. Remote Sensing*, vol. 38, no. 5, pp. 2246–2257, 2000.

[9] A. Stoffelen and D. Anderson, "Scatterometer data interpretation: Estimation and validation of the transfer function CMOD4," *J. Geophys. Res.*, vol. 102, pp. 5767–5780, 1997.

[10] Y. Quilfen and A. Bentamy, "Calibration / validation of ERS-1 scatterometer precision products," in *Proceedings of the International Geosc. and Rem. Sens. Sym. 1994*, Pasadena, USA, 1994, pp. 945–947.

[11] ECMWF, "The description of the evolution of the ECMWF forecasting system and corresponding archive," Technical report, European center for medium-range weather forecast, Reading, United Kingdom, 1999.

[12] W. Alpers and B. Brümmer, "Atmospheric boundary layer rolls observed by the synthetic aperture radar aboard the ERS-1 satellite," *J. Geophys. Res.*, vol. 99, pp. 12 613–12 621, 1994.

[13] A. Stoffelen and D. Anderson, "Scatterometer data interpretation: Measurement space and inversion," *J. Atm. and Ocean Techn.*, vol. 14(6), pp. 1298–1313, 1997.

[14] J. Horstmann, W. Koch, S. Lehner, and R. Tonboe, "Wind retrieval over the ocean using synthetic aperture radar with C-band HH polarization," *IEEE Trans. Geosci. Remote Sensing*, vol. 38, no. 5, pp. 2122–2131, 2000.

[15] P.L. Meadows and P.A. Wright, "ERS-1 SAR analogue to digitalconvertor saturation," in *Proceedings of the CEOS SAR Calibration and Validation Workshop '94*, Michigan, USA, 1994, pp. 24–37.